*36th EPS Conference on Plasma Phys. Sofia, June 29 - July 3, 2009 ECA Vol.**33E**, P-2.172 (2009)*

High speed infrared camera diagnostic for heat flux measurement in NSTX

J-W. Ahn[1], R. Maingi[1], A.L. Roquemore[2], and the NSTX Team

[1]Oak Ridge National Laboratory, Oak Ridge, Tennessee 37831, USA
[2]Princeton Plasma Physics Laboratory, Princeton, New Jersey 08543, USA

1. Introduction

Spherical tokamaks (STs) have smaller plasma volume for a given major radius relative to conventional tokamaks, leading to a higher heat flux density on the divertor plates for a given input power. Heat flux scaling is an important research topic both for extrapolation to next step devices such as NHTX and ITER and for divertor design of planned NSTX upgrades. Two standard frame rate (30Hz) infrared (IR) cameras[1] have been operated to measure heat flux both onto upper and lower divertor tiles in NSTX since 2002[2, 3]. However, due to their limit on the temporal resolution, transient events such as ELMs could not be resolved. These events are of particular interest as they can impose large amount of energy onto the plasma facing components (PFCs) in a short time scale and cause material damages. A new high speed (1.6-6.3kHz) IR camera diagnostic has been recently installed on NSTX and has been successfully commissioned. We report the first results of heat flux measurements from the diagnostic along with technical details.

2. Experimental and measurement technique

NSTX[4, 5] is a low aspect ratio tokamak (R=0.85m, a <0.67m, R/a > 1.27) with machine capabilities of $0.35<B_T<0.55$ toroidal magnetic field, $0.6<I_p<1.2$MA plasma current, $\leq 1.2\times10^{20}$ m^{-3} central density, up to 6MW of neutral beam injected (NBI) power and 6MW of high harmonic fast wave (HHFW) heating system. NBI heating during the I_p ramp was used to minimize volt-second consumption and to extend the pulse length. H-mode plasmas are routinely accessed[6] via good wall conditions, auxiliary heating power, flexible plasma position and shape controls, *etc*. The density rises continuously during the H-mode phase as is typically observed in other tokamak machines.

A Santa Barbara Focalplane (SBF) ImagIR camera with 14 bit dynamic range was installed on NSTX. Detectors of the camera consist of photovoltaic mercury cadmium telluride (HgCdTe) sensor operating in 2-12μm spectral range with 128x128 / 40μs resolution

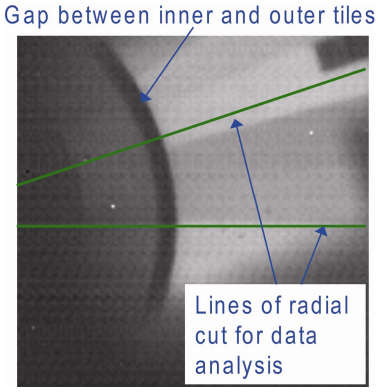

Fig. 1 An IR image of lower divertor tiles viewing from the top of NSTX. Radial profiles of temperature and heat flux are measured along the radial cut line in either horizontal or diagonal direction.

/ pixel pitch. The frame rate is currently 1.6 to 6.3kHz depending on the frame size with flexible integration time of less than 1μs for 128x128 full frame. An integrated vacuum dewar contains liquid nitrogen (LN2) to eliminate IR radiation emitted by the camera itself with hold time of longer than 10 hours. Because of the geometry of the dewar, the camera must be mounted to view horizontally, requiring the implementation of an intermediate mirror mounted on top of the machine to relay the image of lower divertor tiles to the camera lens through a viewing port. Focal length of 25mm of the front lens gives a divertor tile image with spatial resolution of ~6.4mm. Black body source (BBS) calibration against the emission intensity provides a measurement of divertor surface temperature ranging from 20 to 730ºC. The camera hardware and the IR image are very resilient to the strong electromagnetic noise produced by NSTX plasma discharges.

3. Results of surface temperature and heat flux measurement

A typical IR image of the lower divertor tiles are shown in Figure 1. Overlaid, are two radial slices where data analysis occurs. A series of IDL codes were developed to convert the surface emission into temperature and then calculate the heat flux by solving the heat conduction equation. At present, fixed thermal conductivity of the ATJ graphite tiles in the NSTX divertor and a 1-D heat conduction model are being used.-This is the same method applied at DIII-D[7, 8].

Figure 2 shows the measured surface temperature and heat flux at the outer divertor tiles as a function of radius and time for an ELMy H-mode discharge. Also shown in Figure 3 is the time trace of various plasma parameters for the same time window in Figure 2. D_α signal shows repetitive ELMs with short time scales and the rapid peaks at both the temperature and heat flux profiles reflect these ELMs. Note that both the temperature and heat flux peaks from ELMs increase in time as the plasma stored energy (W_{MHD}) increases. In the later stage of the time window, the temperature increase due to an ELM approaches to 400ºC, producing heat flux density of over 150MW/m^2. Figure 4 shows profiles in a narrower time window to examine the effect of individual ELMs in more detail. It is clearly seen that

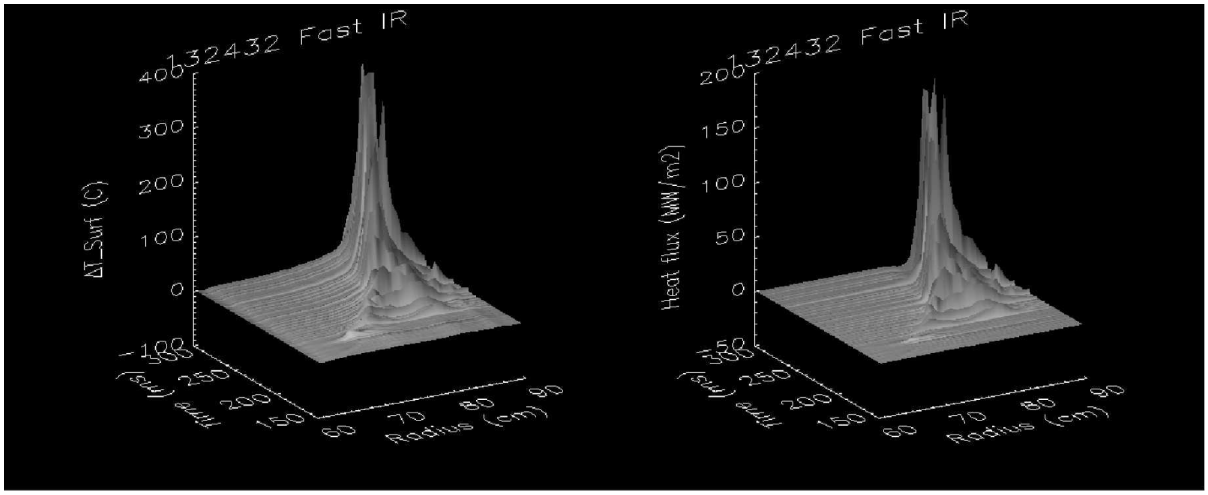

Fig. 2 Measured surface temperature (left) and heat flux (right) profiles as a function of radius and time for an ELMy H-mode plasma at frame rate of 1.6kHz.

both the temperature and heat flux profiles become broadened at the moment of ELM impact with peak temperature and heat flux each increasing by more than a factor of 4 and 10, respectively. A filamentary structure in the profiles is also observed during the ELM. The ELMs push the outer strike point out by 2-3cm momentarily.

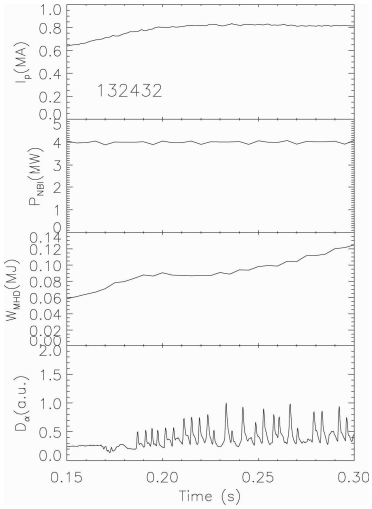

Fig. 3 Time trace of several plasma parameters for the same time window shown in Fig. 2. Note the increase of plasma stored energy (W_{MHD}), which is reflected by the increase of peak temperature and heat flux at the ELM peaks in Fig. 2

In order to validate the fast camera measurements, a comparison with slow (30Hz) IR camera data was made for an ELMy H-mode discharge. The slow IR camera is located on the top of the machine viewing the lower divertor tiles in a different toroidal location displaced by 30 degrees clockwise. The frame rate of the fast IR camera for this discharge was chosen as 1.6kHz. The frequency of ELMs range from 120-180Hz and therefore the slow IR camera with 30Hz frame speed takes an average image over 4-6 ELMs for each frame, while the fast IR camera has enough temporal resolution to resolve individual ELMs. The time slices of the fast camera have been aligned with those of the slow camera and approximately 54 frames (f_{fast}/f_{slow}=1610/30) have been 'time averaged' to generate a frame for each time slice from the slow camera. The agreement is quite good for both the temperature and heat flux profiles.

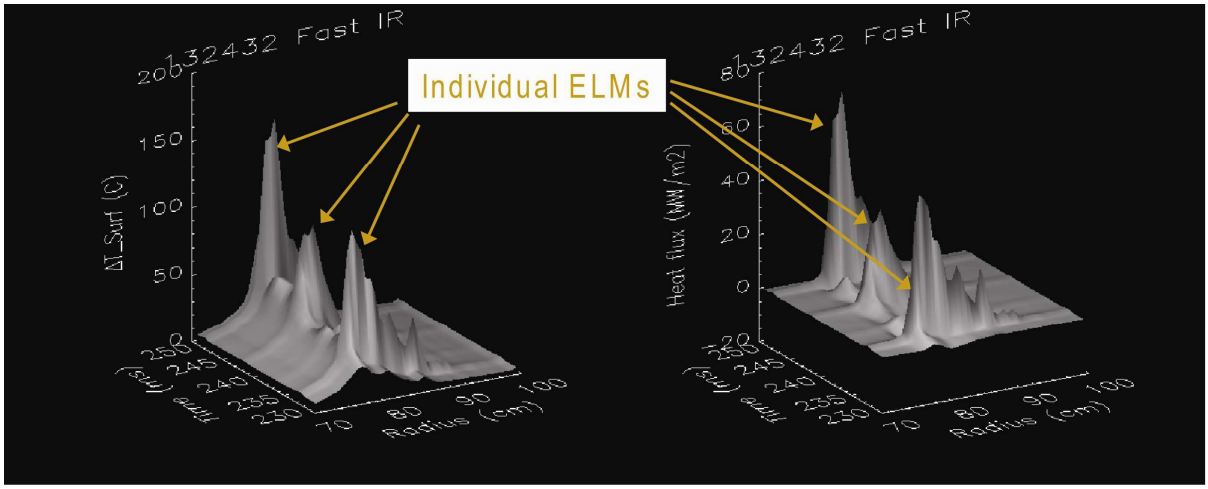

Fig. 4 Measured surface temperature (left) and heat flux (right) profiles as a function of radius and time for individual ELMs with frame rate of 1.6kHz.

The difference in peak heat flux values tends to be larger than the difference in the temperature because a change in temperature in a short time period produces a large heat flux change. However, taking account of the possibility of toroidal asymmetry of heat flux deposition, error bars on the temperature calibration of each camera, and the possibility of slight misalignment of timing sequences for the averaging process, the overall agreement appears good.

4. Summary and conclusion

A new high speed IR camera has been successfully implemented and produced reliable heat flux measurements on the lower divertor tiles in NSTX. High spatial and temporal resolutions enable us to investigate detailed structure of heat flux deposition pattern caused by transient events such as ELMs. A comparison with the data with a slow IR camera viewing the same region of interest shows good agreement between the two independent measurements. Data analysis for various plasma conditions is in progress. This work was supported by the U.S. Department of Energy, contract numbers DE-AC05-00OR22725 and DE-AC52-07NA27344.

References

[1]D. Mastrovito, R. Maingi, H.W.Kugel, and A.L. Roquemore, Review of Sci. Instruments **74** (2003), 5090
[2]R. Maingi, C.E. Bush, R. Kaita, *et. al*, J. of Nucl. Materials (2007), 196
[3]V. Soukhanovskii *et. at.*, Nucl. Fusion (2009), in press
[4]M. Ono, S.M. Kaye, Y.-K.M. Peng, *et. al.*, Nucl. Fusion **40** (2000) 557
[5]S.M. Kaye, M.G. Bell, R.E. Bell, *et. al.*, Nucl. Fusion **45** (2005), S168
[6]R. Maingi, M.G. Bell, R.E. Bell, *et. al.*, Nucl. Fusion **43** (2003), 969
[7]H.S. Carslaw and J.C. Jaeger, Conduction of Heat in Solids, Oxford: Clarendon Press (1959)
[8]D.N. Hill, R. Ellis, W. Ferguson, and D.E. Perkins, Review of Sci. Instrum. **59** (1988), 1878